Advances in Nano Research, *Vol. 14, No. 2 (2023) 127-139*
https://doi.org/10.12989/anr.2023.14.2.127

Proposing a dynamic stiffness method for the free vibration of bi-directional functionally-graded Timoshenko nanobeams

Mohammad Gholami*[1], Mojtaba Gorji Azandariani[2a], Ahmed Najat Ahmed[3a] and Hamid Abdolmaleki[4b]

[1]*Department of Civil Engineering, Yasouj University, Yasouj, Iran*
[2]*Centre for Infrastructure Engineering, Western Sydney University, Sydney, Australia*
[3]*Department of Computer Engineering, College of Engineering and Computer Science, Lebanese French University, Kurdistan Region, Iraq*
[4]*Department of Civil Engineering, Tuyserkan Branch, Islamic Azad University, Tuyserkan, Iran*

(*Received Octpber 6, 2021, Revised July 4, 2022, Accepted August 14, 2022*)

Abstract. This paper studies the free vibration behavior of bi-dimensional functionally graded (BFG) nanobeams subjected to arbitrary boundary conditions. According to Eringen's nonlocal theory and Hamilton's principle, the underlying equations of motion have been obtained for BFG nanobeams. Moreover, the variable substitution method is utilized to establish the structure's state-space differential equations, followed by forming the dynamic stiffness matrix based on state-space differential equations. In order to compute the natural frequencies, the current study utilizes the Wittrick–Williams algorithm as a solution technique. Moreover, the nonlinear vibration frequencies calculated by employing the proposed method are compared to the frequencies obtained in previous studies to evaluate the proposed method's performance. Some illustrative numerical examples are also given in order to study the impacts of the nonlocal parameters, material property gradient indices, nanobeam length, and boundary conditions on the BFG nanobeam's frequency. It is found that reducing the nonlocal parameter will usually result in increased vibration frequencies.

Keywords: bidirectional functionally graded; dynamic stiffness method; Eringen's nonlocal theory, free vibration, nanobeams; state-space differential equations

1. Introduction

Due to the unique properties included in the functionally graded (FG) nanobeams, including low density, high strength, magneto-electro-viscoelastic, thermal resistance, and toughness, they have attracted much attention among scholars and engineers (Ebrahimi *et al.* 2019, Ebrahimi and Haghi 2018, Gao *et al.* 2019, Gorji Azandariani *et al.* 2021b, Talebizadehsardari *et al.* 2020). In the last few years, many research works have been conducted on the different aspects included in FG beams (Amar *et al.* 2017, Belarbi *et al.* 2021, Berghouti *et al.* 2019, Houari *et al.* 2018, Li and Batra 2013, Thai and Vo 2012) Due to technological developments and achievements, functionally graded materials (FGMs) have begun to find their way into micro/nanobeams. Given the great potential of micro/ nanobeams in engineering applications, gaining a proper understanding of their mechanical behavior is of great importance (Chen *et al.* 2022, Chen and Li 2022, Gu *et al.* 2022, Wang *et al.* 2021, Zhang *et al.* 2021). The classic continuum theories suffer from inaccurate predictions done for the mechanical behavior of nanostructures (Hao *et al.* 2022, Huang and Liu 2022, Liu *et al.* 2021, Shi *et al.* 2022). In this regard, a few size-dependent elasticity mechanics have Research Fellow been developed, including the nonlocal theory (Eringen 1983), the theory of modified couple stress (MCS) (Yang *et al.* 2002), Eringen\'s nonlocal elasticity theory (Nejad *et al.* 2018), and the theory of the nonlocal strain gradient (Lim *et al.* 2015).

Due to technological developments and achievements, functionally graded materials have found their way into micro/nanobeams. Given the great potential of micro/ nanobeams in engineering applications, gaining a proper understanding of their mechanical behavior is of great importance (Huang *et al.* 2020, 2021, Wei *et al.* 2021, Zhang *et al.* 2022a). On the other hand, with the advance of nanotechnology, microbeams, whose thickness is generally on the order of microns and sub-microns, have been widely used in many applications of microdevices (Belarbi *et al.* 2021). Micro-electro-mechanical systems are a technology that, in its most general form, can be defined as devices and structures made using microfabrication techniques in its most general form. The critical physical dimensions of micro-electro-mechanical systems devices can vary from well below one micron on the lower end of the dimensional spectrum, all the way to several millimeters (Chen *et al.* 2022, Hu *et al.* 2022, Shan *et al.* 2022, Zhang *et al.* 2022b). While the functional elements of micro-electro-mechanical systems are miniaturized structures, sensors, actuators, and microelectronics, the most notable elements are the microsensors and microactuators (Bai *et al.* 2021, Yuan *et al.* 2022, Zhou *et al.* 2022). However, it is experimentally proved that the size effect also becomes important for the mechanical behavior of microstructures when the dimensions of structures become on the order of microns

*Corresponding author, Assistant Professor,
E-mail: m.gholami@yu.ac.ir
[a] Ph.D.
[b] Ph.D. Student

Copyright © 2023 Techno-Press, Ltd.

ISSN: 2287-237X (Print), 2287-2388 (Online)

and sub-microns. Due to this fact, it is inevitable to consider the size effect in analyzing the mechanical behavior of microstructures. At the same time, since controlled experiments in microscale are both difficult and expensive, the development of appropriate mathematical models for microstructures is an important issue concerning an approximate analysis of microstructures (Karami *et al.* 2018, 2019, Karami and Janghorban 2019).

Gao *et al.* (2019) investigated non-linear thermal buckling of bi-directional functionally graded beams in the theoretical frameworks of nonlocal strain graded theory. This study was used a higher-order shear deformation theory that contains a physical neutral surface to derive the size-dependent governing equations hybrid with Hamilton's principle and the von Kármán geometric nonlinearity. Also, a parametric study is performed in detail after verifying the analysis, especially for the effects of a nonlocal parameter, a strain gradient length scale parameter, and the ratio of the two on the critical thermal buckling temperature of beams. Ebrahimi and Barati (2018) provide an analytical solution to the buckling governing equations of functionally graded piezoelectric (FGP) nanobeams obtained using a developed third-order shear deformation theory. Employing Hamilton's principle, the nonlocal governing equations of an FG nanobeam made of piezoelectric materials are obtained, and they were solved by applying a Navier-type analytical solution. Ebrahimi and Barati (2018) validated the present model's accuracy by comparing it with nonlocal Timoshenko FG beams. Aydogdu *et al.* (2018) studied the vibration of axially functionally graded nano-rods and beams. The Ritz method with algebraic polynomials and stress gradient elasticity theory with the nonlocal effects formulated the problems.

Also, the nonlocal parameter was assumed to change linearly or quadratically along the length of the nano-structure. Frequencies are compared to constant nonlocal parameter cases, and considerable differences are observed between constant and variable nonlocal parameter cases. Mode shapes in various cases are depicted to explain the effects of axial grading. Luat *et al.* (2021) investigated the bending, free vibration, and buckling analysis of a novel bi-functionally graded sandwich nanobeam via a nonlocal refined simple shear deformation theory. The novel sandwich beam included one ceramic core and two different functionally graded face sheets. Eringen's nonlocal elastic theory was utilized in cooperation with a refined simple shear deformation theory and Hamilton's principle to derive the equations of motion. A closed-form solution based on Navier's technique is used to solve the equations of motion of supported nanobeams. Also, in this study, the results were compared with existing solutions to evaluate the accuracy of the proposed theory. Zidi *et al.* (2017) proposed a novel, simple higher-order shear deformation theory for bending and free vibration analysis of functionally graded (FG) beams. In this method, equations of motion were obtained via Hamilton' principle. Zidi *et al.*'s (2017) analytical equations for the bending and free vibration analysis were presented for simply supported beams. The numerical results compared with those of other higher-order shear deformation beam theories were obtained and validated.

The buckling behavior and the vibration behavior of FG micro/nanobeams have been investigated in many studies. For example, in a study, the FG Timoshenko microbeams' free vibration was investigated according to the MCS theory. The free vibrations of FG microbeams were analyzed using the theory of the strain gradient. A group of researchers has studied the nonlinearity of the free vibration in the FG microbeams using the theory of MCS (Ke *et al.* 2012). By applying the nonlocal theory, a finite element formulation was proposed to analyze the free vibrations in the FG nanobeams (Nejad *et al.* 2017, Sanjay Anandrao *et al.* 2012, Setoodeh and Rezaei 2017). In these works, the static buckling behavior in the FG nanobeams depended on size was also studied using the nonlocal continuum model. In another work, the bending/buckling behaviors of FG nanobeam have been examined through an analytical approach concerning nonlocal theory based on Timoshenko and Euler Bernoulli beam (Simsek and Yurtcu 2013). In addition, the vibrations were also examined in the simply supported (SS) Timoshenko FG nanobeams applying the MCS theory (Rahmani and Pedram 2014). Through an analytical study, the size-dependent bending/ buckling behaviors were examined in the FG nanobeams considering the effects induced by thickness stretching (Chaht *et al.* 2015, Rabhi *et al.* 2020). Moreover, in many other types of research, the vibration behavior and the buckling behavior of the FG micro/nanobeams have been investigated (Chaht *et al.* 2015, Rahmani *et al.* 2017, Tagrara *et al.* 2015).

One of the critical issues in structural engineering is the non-linear bending of the beam exposed to very large displacements. The beam bending behavior is in a non-linear regime when the ends of a beam subjected to large transverse loads are axially immovable because of axial tension induced by a large deflection. Lately, many researchers have been trying to investigate the non-linear behavior of FG beams. Through a study conducted on the non-linear behavior in the FG structures, the size dependency of non-linear vibrations has been investigated in the FG microbeams using the Casimir force, combined electrostatic force, and temperature changes (Jia *et al.* 2015). In another study, the non-linear bending behavior was investigated in the tapered FG beam subjected to the thermal/mechanical loads (Niknam *et al.* 2014, Zenkour and Abouelregal 2015). In a different work, an exact solution was proposed by some scholars to solve the non-linear forced vibrations in the FG nanobeams by taking into account the surface effect (Akbaş 2019). The non-linear vibrations of the size-dependent beam were investigated according to Eringen's nonlocal theory and the non-linear geometric theory (Ahouel *et al.* 2016, Şimşek, 2014). In addition to the done research, some other investigations were also conducted to study the non-linear vibration of the FG micro/nanobeams (Setoodeh and Rezaei 2017, Şimşek 2016).

Nanotechnology has prominent advantages for developers who are working to make people's lives easier. This relatively new technology has led to the construction of subatomic or nanostructured structures that have a variety of applications in medicine, electronics, mechanics, solar cells, etc. Therefore, in the field of mechanical

engineering, the study of the behavior of nanoscale structures has been of great importance. Three different methods are suggested to predict the mechanics of these structures (i.e., experimental tests, molecular dynamics (MD) simulation, and non-classical theories). Experimental tests and MD simulations have more complexity compared to non-classical theories, which has led to the development of this category of theories in recent years. Because in engineering, reducing the complexity of computing, which leads to time and cost savings, is important.

A review of the history of the above research clearly shows that no attention has been paid to the mechanical behavior of nanobeams with geometric nonlinearity and to the author's knowledge, no published work on eringen's nonlocal theory for non-linear free vibration of bi-directional functionally graded Timoshenko nanobeams there is no pair. Accordingly, in the present study, the impact of the nonlinearity related to geometry is thoroughly examined on the free vibration of BFG nanobeams applying Eringen's nonlocal theory. In order to simplify the formulation, the problem formulas are derived according to the physical middle surface. The Hamilton principle is employed to determine governing partial differential equations as well as boundary conditions. Moreover, the dynamic stiffness method (DSM) and direct iterative method are applied to solve governing equations. Present results for non-linear static deflection were compared with previously published results in order to validate the present formulation. The impacts of the nonlocal factors, beam length and material property gradient on the non-linear free vibration of BFG nanobeams are investigated. It is observed that these parameters are vital in the value of the non-linear free vibration of the BFG nanobeam.

As can be seen in the literature of this field of study, the dynamic stiffness method (DSM) commonly represents an exact solution method. In addition, the DSM, unlike the finite element method, allows a whole uniform structural member to be represented as a single element regardless of its length. This will result, as a consequence, in a significant reduction in the total magnitude of degrees of freedom applied to the dynamic analysis while reducing the computation cost. As far as the authors know, there have been no studies focusing on employing the DSM to find a solution to the vibration problem of BFG nanobeam. In the present paper, the dynamic stiffness method is developed for free vibration of BFG Timoshenko nanobeams by employing Eringen's non-local theory.

2. Experimental

The material properties of the FG beam gradually change along their thickness direction, while the material properties of bi-directional functionally graded (BFG) nanobeams change along both length and thickness of the nanobeam (Fig. 1(a)). It is worths mentioning that the studies, as mentioned earlier, are related to FG micro/ nanobeams. The reported results regarding the BFG micro/ nanobeams are not remarkable. Eringen's nonlocal theory was developed based on the differential quadrature method (DQM) using the Euler in a few studies on the BFG

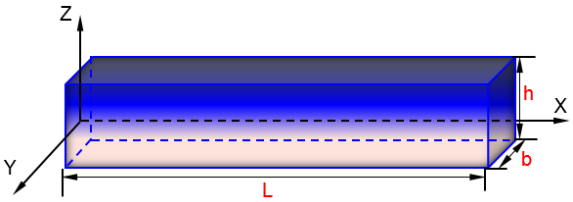

(a) variation in mechanical properties

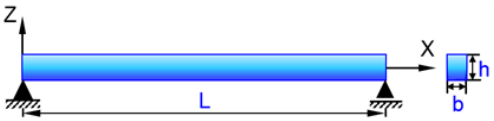

(b) physical neutral surface and geometric mid-surface

Fig. 1 Bi-directional functionally graded (BFG) nanobeam

nanobeams considering the buckling, bending, and vibration behaviors–Bernoulli theory. The buckling and vibration behaviors were also analyzed in the BFG porous tapered micro/nanobeams and imperfect BFG porous micro /nanobeams applying theories of Euler–Bernoulli and Timoshenko beams (Gholami *et al.* 2021, Gorji Azandariani *et al.* 2021d, Rousta *et al.* 2021, Rousta and Azandariani 2022, Usefvand *et al.* 2021, Vaziri *et al.* 2021).

2.1 Functionally graded materials

Assum a BFG nanobeam with a length defined as L and a rectangular cross-section defined as $b \times h$ (b = width and h = height), and with simple immovable supports at both ends (Fig. 1(b)). In Fig. 1, a functionally graded (FG) nanobeam of length L, width b, and thickness h is presented. The x_1 = X, x_2 = Y, and x_3 = Z coordinates are selected along the length, width, and thickness of the FG nanobeam, respectively. We supposed that the FG nanobeam is made of two dissimilar materials, and the effective material properties of the FG nanobeam vary continuously in the thickness direction (in the z-direction). Here, to simplify the calculations, the assumption is that Poisson's ratio v is constant. Moreover, mass density ρ, as well as elasticity modulus E, is defined as follows (Nejad and Hadi 2016):

$$E(x, z_{ms}) = e^{N_x \frac{x}{L}} \left[(E_c - E_m) \left(\frac{z_{ms}}{h} + \frac{1}{2} \right)^{N_z} + E_m \right] \quad (1)$$

$$\rho(x, z_{ms}) = e^{N_x \frac{x}{L}} \left[(\rho_c - \rho_m) \left(\frac{z_{ms}}{h} + \frac{1}{2} \right)^{N_z} + \rho_m \right] \quad (2)$$

where m is the metallic constituent, c is the ceramic constituent, N_x and N_z indicate the gradient parameters dictating the alteration profile of the material along the thickness direction and length direction of the nanobeam, respectively.

2.2 Eringen's nonlocal theory

Eringen's nonlocal theory (Eringen 1983) assumes that the stress tensor matrix at any point of x in the material domain is dependent on two factors: **(i)** the strain tensor

matrix corresponding to point *x*, **(ii)** strain tensor matrix at all of the rest of points in the domain. It is consistent with experimental data reported in the literature based on the lattice dynamics and the atomic theory. Based on the mentioned theory, components of the tensor matrix of the nonlocal stress σ_{ij} (x) at an arbitrary point of x in the homogeneous elastic body could be defined by the following equation:

$$\sigma_{ij}(x) = \int_{\Omega}^{l} \alpha(|x' - x|, \tau) t_{ij}(x') d\Omega(x') \tag{3}$$

where $t_{ij}(x')$ is the component for the classic local stress-tensor at point x, a relationship can be defined between classic local stress-tensor and linear tensor matrix of the strain ε_{kl} using the fundamental equations for a Hookean material:

$$t_{ij} = c_{ijkl}\varepsilon_{kl} \tag{4}$$

In Eq. (3), α is the kernel function known as nonlocal modulus, which depends on two variables $|x'-x|$ defined as the distance in Euclidean form and τ that is determined as follows:

$$\tau = \frac{e_0 a}{l} \tag{5}$$

where τ represents the ratio of a characteristic internal length (e.g., granular distance, lattice parameter), a is a characteristic internal length (e.g., lattice parameter, granular distance), and l is a characteristic external length (e,g., crack length, wavelength) related to each material using an adjusting constantly, e_0, the e_0 magnitude is estimated through two ways: **(i)** by fitting the dispersion curves of plane waves to the dispersion curves of atomic lattice dynamics or, **(ii)** experimentally.

According to a study conducted by Eringen, the nonlocal integral fundamental equation (Eq. (3)) could be expressed in differential form in the following way if the appropriate kernels function is chosen:

$$(1 - (e_0 a)^2 \nabla^2)\sigma_{kl} = t_{kl} \tag{6}$$

where ∇^2 indicates the Laplacian operator. For one dimension, it is possible to simplify the nonlocal constitutive relation (Eq. (6)) for an elastic material as follows:

$$\sigma_{xx} - (e_0)^2 \frac{\partial^2 \sigma_{xx}}{\partial x^2} = E\varepsilon_{xx} \tag{7a}$$

$$\sigma_{xz} - (e_0)^2 \frac{\partial^2 \sigma_{xz}}{\partial x^2} = G\gamma_{xz} \tag{7b}$$

where E, G, σ_{xx}, σ_{xz}, ε_{xx}, and γ_{xz} are the elasticity modulus, shear modulus, normal axial stress, shear stress, axial and shear strain, respectively.

3. The governing equation and boundary conditions

The current analysis utilizes the Timoshenko beam theory. Displacements of u_1, u_2, and u_3 along the X, Y, and Z directions of a point on the cross-section can be expressed as follows (Rahmani and Pedram 2014):

$$\begin{aligned} u_1(x,z,t) &= u(x,t) - z_c\phi(x,t) \\ u_2(x,z,t) &= 0 \\ u_3(x,z,t) &= w(x,t) \end{aligned} \tag{8}$$

where $u(x,t)$ and $w(x,t)$ are the axial and transverse displacements of a point on the beam mid-surface, respectively, ϕ (x,t) signifies the cross-section flexural rotations at any point on the neutral beam axis. t stands for time. The strains are expressed by following Eq. (9) (Rahmani and Pedram 2014):

$$\begin{aligned} \varepsilon_{xx} &= \frac{\partial u}{\partial x} - z_c \frac{\partial \phi}{\partial x} \\ \varepsilon_{xz} &= \frac{1}{2}\left(\frac{\partial w}{\partial x} - \phi\right) \end{aligned} \tag{9}$$

Note the shear strain $\gamma_{xz} = 2\varepsilon_{xz}$.

The following equations provide the normal and shear stresses of the beam when it is assumed that the material of the FGB follows Hooke's law:

$$\sigma_{yy} = E(z)\varepsilon_{yy}, \qquad \tau_{yy} = G(z)\gamma_{yy} \tag{10}$$

The potential energy V corresponding to the BFG nanobeams is determined by the use of Eq. (9) as follows (Rahmani and Pedram 2014):

$$\begin{aligned} V &= \frac{1}{2}\int_0^L \int_A (\sigma_{xx}\varepsilon_{xx} + 2\sigma_{xz}\varepsilon_{xz}) dA dy = \\ &\frac{1}{2}\int_0^L h\left[N_{xx}\left(\frac{\partial u}{\partial x}\right) - M_{xx}\frac{\partial \theta}{dx} + Q_{xz}\left(\frac{\partial w}{\partial x} - \phi\right)\right] dx \end{aligned} \tag{11}$$

where the resultant normal force N_{xx}, shearing force Q_x, and flexural moment M_{xx} are expressed in the form of as follows:

$$N_{xx} = \int_A \sigma_{xx} dA \tag{12a}$$

$$M_{xx} = \int_A z_c \sigma_{xx} dA \tag{12b}$$

$$Q_{xz} = \int_A \sigma_{xz} dA \tag{12c}$$

The equation below can be utilized for estimating the kinetic energy of the system considering both longitudinal displacement and transverse displacement:

$$\begin{aligned} T &= \frac{1}{2}\int_0^L \int_A P(x.z)\left[\left(\frac{\partial u_1}{\partial t}\right)^2 + \left(\frac{\partial u_3}{\partial t}\right)^2\right] dA dx \\ &= \frac{1}{2}\int_0^L \begin{bmatrix} I_0 e^{B\frac{x}{L}}\left(\left(\frac{\partial w}{\partial t}\right)^2 + \left(\frac{\partial u}{\partial t}\right)^2\right) \\ -2I_1 e^{B\frac{x}{L}}\left(\frac{\partial \phi}{\partial t}\right)\left(\frac{\partial u}{\partial t}\right) + I_2 e^{B\frac{x}{L}}\left(\frac{\partial \phi}{\partial t}\right)^2 \end{bmatrix} dx \end{aligned} \tag{13}$$

where:

$$\begin{aligned} &(I_0, I_1, I_2) = \\ &b\int_{-\frac{h}{2}}^{\frac{h}{2}} \left(1, z, z^2\right)\left[(\rho_c - \rho_m)\left(\frac{z}{h} + \frac{1}{2}\right)^{N_z} + \rho_m\right] dz \end{aligned} \tag{14}$$

The following equation defines Hamilton's principle:

$$\delta\int_{t_1}^{t_2}(T-V)dt=0 \tag{15}$$

The governing equations can be determined by substituting the expressions for V (in Eq. (11)) and T (in Eq. (13)) into Eq. (15), performing a partial integration concerning x and t, and finally utilizing the fundamental lemma of the calculus of variations as follows:

$$\delta_u \Rightarrow \frac{\partial N_{xx}}{\partial x}=-I_0 e^{B\frac{x}{L}}\frac{\partial^2 u}{\partial t^2}+I_1 e^{B\frac{x}{L}}\frac{\partial^2 \phi}{\partial t^2} \tag{16a}$$

$$\delta_\phi \Rightarrow Q_{xz}+\frac{\partial M_{xx}}{\partial x}=I_1 e^{B\frac{x}{L}}\frac{\partial^2 u}{\partial t^2}-I_2 e^{B\frac{x}{L}}\frac{\partial^2 \phi}{\partial t^2} \tag{16b}$$

$$\delta_w \Rightarrow \frac{\partial Q_{xx}}{\partial x}=-I_0 e^{B\frac{x}{L}}\frac{\partial^2 w}{\partial t^2} \tag{16c}$$

Using Eqs. (7a), (7b), (9), (10), and (12), are determined the force-displacement and moment–displacement relations of the nonlocal Timoshenko beam theory, presented as follows:

$$\begin{aligned}&N_{xx}-\mu\frac{\partial^2 N_{xx}}{\partial x^2}\\&=-\int_A^g E(x,z)\left[\frac{\partial u}{\partial x}-z\frac{\partial^2 w}{\partial x^2}\right]dA\\&=-A_0 e^{B\frac{x}{L}}\frac{\partial u}{\partial x}+A_1 e^{B\frac{x}{L}}\frac{\partial \phi}{\partial x}\end{aligned} \tag{17a}$$

$$\begin{aligned}&Q_{xz}-\mu\frac{\partial^2 Q_{xz}}{\partial x^2}\\&=-\int_A^g G(x,z)\left(\frac{\partial w}{\partial x}-\phi\right)dA\\&=-A_3 e^{B\frac{x}{L}}\left(\frac{\partial w}{\partial x}-\phi\right)\end{aligned} \tag{17b}$$

$$\begin{aligned}&M_{xx}-\mu\frac{\partial^2 M_{xx}}{\partial x^2}\\&=\int_A E(x,z)\left[z\frac{\partial u}{\partial x}-z^2\frac{\partial \phi}{\partial x}\right]\\&=A_1 e^{B\frac{x}{L}}\frac{\partial u}{\partial x}-A_2 e^{B\frac{x}{L}}\frac{\partial \phi}{\partial x}\end{aligned} \tag{17c}$$

where the shear strain $\mu=e_0^2$.

Moreover, the following equations define the stiffness coefficients in the abovementioned equations:

$$\begin{aligned}&(A_0,A_1,A_2)\\&=b\int_{-\frac{h}{2}}^{\frac{h}{2}}(1,z,z^2)\left((E_c-E_m)\left(\frac{z}{h}+\frac{1}{2}\right)^{N_z}+E_m\right)dz\end{aligned} \tag{18a}$$

$$A_3=\frac{bK_s}{2(1+\nu)}\int_{-\frac{h}{2}}^{\frac{h}{2}}\left[(E_c-E_m)\left(\frac{z}{h}+\frac{1}{2}\right)^{N_z}+E_m\right]dz \tag{18b}$$

Using the size-dependent equilibrium Eqs. (16a)-(16c), it is possible to obtain the axial force (17a), shear force (17b), and the moment (17c), as follows:

$$\begin{aligned}&Q_{xz}=-A_3 e^{B\frac{x}{L}}\left(\frac{\partial w}{\partial x}-\phi\right)+\\&\mu\left(-I_0 e^{B\frac{x}{L}}\frac{\partial^3 w}{\partial x\partial t^2}-\frac{B}{L}I_0 e^{B\frac{x}{L}}\frac{\partial^2 w}{\partial t^2}\right)\end{aligned} \tag{19a}$$

$$\begin{aligned}&N_{xx}=-A_0 e^{B\frac{x}{L}}\frac{\partial u}{\partial x}+A_1 e^{B\frac{x}{L}}\frac{\partial \phi}{\partial x}\\&+\mu(-I_0 e^{B\frac{x}{L}}\frac{\partial^3 u}{\partial x\partial t^2}-\frac{B}{L}I_0 e^{B\frac{x}{L}}\frac{\partial^2 u}{\partial t^2}+\\&I_1 e^{B\frac{x}{L}}\frac{\partial^3 \phi}{\partial x\partial t^2}+\frac{B}{L}I_1 e^{B\frac{x}{L}}\frac{\partial^2 \phi}{\partial t^2})\end{aligned} \tag{19b}$$

$$\begin{aligned}&M_{xx}=M_{xx}=A_1 e^{B\frac{x}{L}}\frac{\partial u}{\partial x}-A_2 e^{B\frac{x}{L}}\frac{\partial \phi}{\partial x}\\&+\mu(I_1 e^{B\frac{x}{L}}\frac{\partial^3 u}{\partial x\partial t^2}+\frac{B}{L}I_1 e^{B\frac{x}{L}}\frac{\partial^2 u}{\partial t^2}-\\&I_2 e^{B\frac{x}{L}}\frac{\partial^3 \phi}{\partial x\partial t^2}-\frac{B}{L}I_2 e^{B\frac{x}{L}}\frac{\partial^2 \phi}{\partial t^2}+I_0 e^{B\frac{x}{L}}\frac{\partial^2 w}{\partial t^2})\end{aligned} \tag{19c}$$

Harmonic oscillation is assumed as the following:

$$\begin{aligned}U_0(x,t)&=U(x)e^{i\omega t}\\W_0(x,t)&=W(x)e^{i\omega t}\\\phi_0(x,t)&=\phi(x)e^{i\omega t}\end{aligned} \tag{20}$$

where U(y), W(y) and ϕ(y), respectively, represent the amplitudes of V_0, W_0, and ϕ_0. Also, ω indicates circular frequency. The variables V_0, W_0, and ϕ_0 are defined as follows:

$$\begin{aligned}W_0&=we^{\beta\frac{x}{l}}\\U_0&=Ue^{\beta\frac{x}{l}}\\\phi_0&=\phi e^{\beta\frac{x}{l}}\end{aligned} \tag{21}$$

Thus,

$$\begin{aligned}w'.e^{\beta\frac{x}{l}}&=W_0'-\beta\frac{x}{l}W_0\\\upsilon'.e^{\beta\frac{x}{l}}&=U_0'-\beta\frac{x}{l}U_0\\\phi'.e^{\beta\frac{x}{l}}&=\phi_0'-\beta\frac{x}{l}\phi_0\end{aligned} \tag{22}$$

Using Eqs. (20), (21), and (22), it is possible to express the axial force (19a), shear force (19b), and the moment (19c) as follows:

$$\begin{aligned}&N=-A_0\left[U'-\frac{B}{L}U\right]+A_1\left[\phi'-\frac{B}{L}\phi\right]+\\&\mu\left(I_0\omega^2\left[U'-\frac{B}{L}U\right]+\frac{B}{L}I_0\omega^2 U\right)-\\&\mu\left(I_1\omega^2\left[\phi'-\frac{B}{L}\phi\right]-\frac{B}{L}I_1\omega^2\phi\right)\end{aligned} \tag{23a}$$

$$\begin{aligned}&Q=-A_3\left[W'-\frac{B}{L}W\right]+A_3\phi+\\&\mu I_0\omega^2\left(\frac{B}{L}+\left[W'-\frac{B}{L}W\right]\right)\end{aligned} \tag{23b}$$

$$M=A_1\left[U'-\frac{B}{L}U\right]-A_2\left[\phi'-\frac{B}{L}\phi\right]+ \tag{23c}$$

$$\mu\left(I_1\omega^2\left[\frac{B}{L}U-U'\right]-\frac{B}{L}I_1\omega^2U\right)+$$
$$\mu\left(I_2\omega^2\left[\phi'-\frac{B}{L}\phi\right]+\frac{B}{L}I_2\omega^2\phi-I_0\omega^2W\right)$$

Using the Eqs (23), (16a), (16b), and (16c), the state-space equation can obtain as:

$$\frac{\partial v}{\partial y}=Av \tag{24}$$

where v represents the state-space variable and $v=[W,\ \phi,\ V,\ Q,\ M,\ N]^T$ where S, M, and F, respectively, indicate the amplitudes of the shear force, bending moment, and axial force. Also, we can express Matrix A is obtained as follows:

$$A=\begin{bmatrix} b_1 & b_2 & 0 & b_3 & 0 & 0\\ b_4 & b_5 & b_6 & 0 & b_7 & b_8\\ b_9 & b_{10} & b_{11} & b_{12} & 0 & b_{13}\\ \omega^2I_0 & 0 & 0 & 0 & 0 & 0\\ 0 & \omega^2I_2 & -\omega^2I_1 & -1 & 0 & 0\\ 0 & -\omega^2I_1 & \omega^2I_0 & 0 & 0 & 0 \end{bmatrix} \tag{25}$$

where:

$$b_1=\frac{-A_3\left(\frac{B}{L}\right)}{(-A_3+\mu I_0\omega^2)},\quad b_2=\frac{A_3}{(A_3-\mu I_0\omega^2)}$$
$$b_3=\frac{1}{(-A_2+\mu I_0\omega^2)},\quad b_4=\frac{-\mu I_0\omega^2[A_1-\mu I_0\omega^2]}{D_1}$$

$$b_5=\frac{\left[\mu\frac{B}{L}I_1\omega^2-A_1\frac{B}{L}-\mu\frac{B}{L}I_1\omega^2\right][A_1-\mu I_1\omega^2]}{D_1}-\frac{\left[A_2\frac{B}{L}-\mu\frac{B}{L}I_2\omega^2+\mu\frac{B}{L}I_2\omega^2\right][-A_0+\mu I_0\omega^2]}{D_1}$$

$$b_6=\frac{\left[A_0\frac{B}{L}-\mu\frac{B}{L}I_0\omega^2+\mu\frac{B}{L}I_0\omega^2\right][A_1-\mu I_1\omega^2]}{D_1}-\frac{\left[\mu\frac{B}{L}I_1\omega^2-\frac{B}{L}A_1-\mu\frac{B}{L}I_1\omega^2\right][-A_0+\mu I_0\omega^2]}{D_1}$$

$$b_7=\frac{[\mu I_0\omega^2-A_0]}{D_1},\quad b_8=\frac{-[A_1-\mu I_1\omega^2]}{D_1}$$
$$b_9=\frac{\mu I_0\omega^2[A_2-\mu I_2\omega^2]}{D_2}$$

$$b_{10}=\frac{\left[\mu\frac{B}{L}I_1\omega^2-A_1\frac{B}{L}-\mu\frac{B}{L}I_1\omega^2\right][\mu I_2\omega^2-A_2]}{D_2}-\frac{\left[\frac{B}{L}A_2-\mu\frac{B}{L}I_2\omega^2+\mu\frac{B}{L}I_2\omega^2\right][A_1-\mu I_1\omega^2]}{D_2}$$

$$b_{12}=\frac{[A_1-\mu I_1\omega^2]}{D_2},\qquad b_{13}=\frac{[A_2-\mu I_2\omega^2]}{D_2}$$

$$b_{11}=\frac{\left[A_0\frac{B}{L}-\mu\frac{B}{L}I_0\omega^2+\mu\frac{B}{L}I_0\omega^2\right][\mu I_2\omega^2-A_2]}{D_2}-\frac{\left[\mu\frac{B}{L}I_1\omega^2-A_1\frac{B}{L}-\mu\frac{B}{L}I_1\omega^2\right][A_1-\mu I_1\omega^2]}{D_2}$$

where:

$$D_1=[A_2-\mu I_2\omega^2][A_0-\mu I_0\omega^2]-[A_1-\mu I_1\omega^2]^2 \tag{26a}$$

$$D_2=[A_0-\mu I_0\omega^2][\mu I_2\omega^2-A_2]+[A_1-\mu I_1\omega^2]^2 \tag{26b}$$

In the case of ignoring the nonlocal parameter, μ, in Eqs. (25) and (26), it would be possible to recover Matrix A given in Deng *et al.*'s work (Deng and Cheng 2016). Using Eq. (24) as well as the precise integration method (Deng and Cheng 2016):

$$X=T.X_0 \tag{27}$$

where X_0 represents the structure's initial state vector, and T indicates the transfer matrix, which is obtained as shown below:

$$T=e^{A.L} \tag{28}$$

According to the procedure proposed in (Zhu and Law 2001), it is possible to obtain the element dynamic stiffness matrix K as follows:

$$\begin{bmatrix}F_L\\F_R\end{bmatrix}=\begin{bmatrix}K_{11} & K_{12}\\K_{21} & K_{22}\end{bmatrix}\begin{bmatrix}X_L\\X_R\end{bmatrix} \tag{29}$$

where,

$$K_{11}=-T_{12}^{-1}.T_{11},K_{12}=T_{12}^{-1}$$
$$K_{21}=-T_{21}+T_{22}T_{12}^{-1}.T_{11},K_{22}=-T_{12}^{-1}.T_{22} \tag{30}$$

4. Numerical results

This section has two subsections, one dealing with verifying the presented non-local model by comparing its results to the results from previous studies (Azandariani *et al.* 2022; Gorji Azandariani *et al.* 2022a, 2021c, b; a, 2022b; Gorji Azandariani and Gholami 2022a). One presents the effects of nonlocality, the length of the nanobeam, the boundary conditions, and the material distribution on the BFG nanobeam's frequency. It is possible to estimate the relevant boundary conditions similarly. That is, for a clamped - clamped (CC) and Simple – simple (SS) BFG microbeam (Table 1):

$$u=w=\phi=0\quad at\ x=0$$
$$u=w=\phi=0\quad at\ \ x=L\quad \text{for (CC)} \tag{31a}$$

$$u=w=0\quad at\ x=0$$
$$u=w=0\quad at\ \ x=L\quad \text{for (SS)} \tag{31b}$$

4.1 Validation of the model

In this section, two different comparison studies are used to evaluate the reliability of the proposed model and the obtained results; the comparisons are related to the frequency ratios of a linear simply supported (SS) conventional FG nanobeam Rahmani & Pedram (2014) and Eltaher *et al.* (2012) and a linear clamped-clamped (CC) BFG nanobeam. First, comparing the current results with

Table 1 Types of the considered boundary conditions

Boundary condition type	Conditions	
	x= 0	x= L
Simple – simple	$u = w = 0$	$u = w = 0$
Clamped – clamped	$u = w = \phi = 0$	$u = w = \phi = 0$

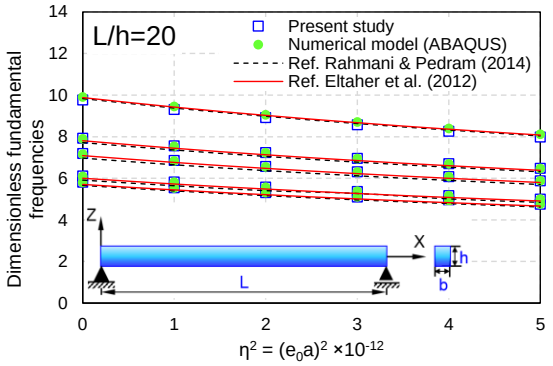

(a)

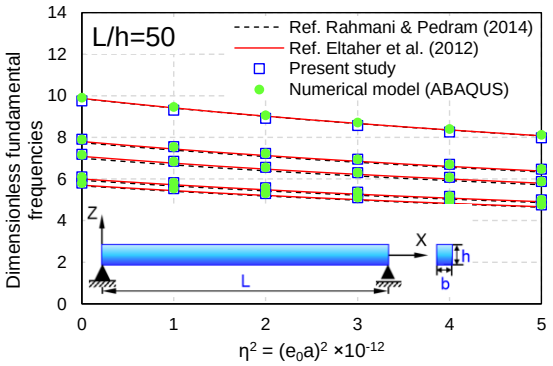

(b)

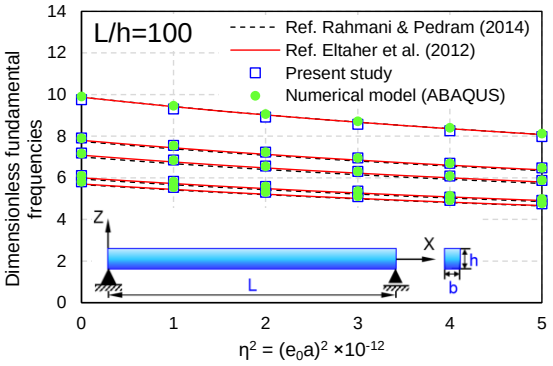

(c)

Fig. 2 Comparison of non-dimensionless fundamental natural frequencies of the present study with Rahmani & Pedram (2014), Eltaher *et al.* (2012), and numerical model (ABAQUS)

the findings in Refs. Rahmani & Pedram (2014) and Eltaher *et al.* (2012) is performed.

When both effects of the FG gradient index along the axis N_x and nonlinear terms are ignored, the non-dimensionless frequencies of the conventional FG microbeams Rahmani & Pedram (2014) and Eltaher *et al.* (2012) are obtained and exhibited in Fig. 2. Table 2 to 6 list the dimensionless frequencies for simply supported Timoshenko

Table 2 Comparison of non-dimensionless fundamental natural frequencies of simply supported nanobeams for N_z = 0

L/h	η^2= $(e_0a)^2$ ×10^{-12}	Non-dimensionless fundamental frequencies $(\hat{\omega}_1 = \omega_1 L^2\sqrt{\rho_a A/E_a I})$			
		Present study	Ref. Rahmani & Pedram (2014)	Ref. Eltaher *et al.* (2012)	Numerical model (ABAQUS)
20	0	9.7611	9.8296	9.8797	7.8960
	1	9.3107	9.3777	9.4238	7.5357
	2	8.9173	8.9829	9.0257	7.2212
	3	8.5700	8.6341	8.6741	6.9432
	4	8.2604	8.3230	8.3607	6.6956
	5	7.9819	8.0433	8.0789	6.4728
50	0	9.7539	9.8631	9.8724	7.9005
	1	9.3042	9.4097	9.4172	7.5405
	2	8.9122	9.0136	9.0205	7.2263
	3	8.5659	8.6636	8.6700	6.9488
	4	8.2572	8.3515	8.3575	6.7013
	5	7.9795	8.0708	8.0765	6.4787
100	0	9.7515	9.8680	9.8700	7.9007
	1	9.3032	9.4143	9.4162	7.5412
	2	8.9114	9.0180	9.0197	7.2271
	3	8.5654	8.6678	8.6695	6.9496
	4	8.2568	8.3555	8.3571	6.7021
	5	7.9792	8.0747	8.0762	6.4796

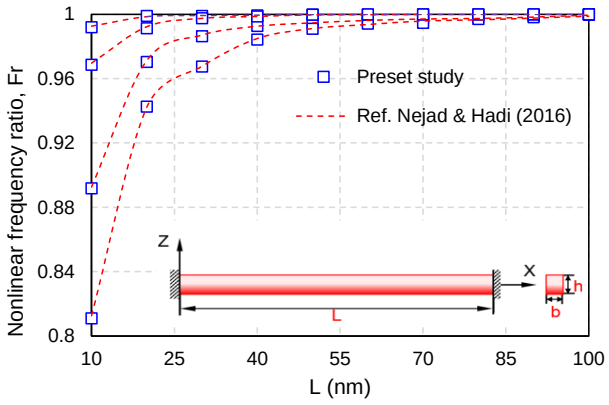

Fig. 3 Comparison of Nonlinear frequency ratio of the present study with Nejad & Hadi (2016)

Timoshenko FG nanobeam with L = 10000 nm and b = 1000 nm for different amounts of gradient index, nonlocal parameter, and slender ratio. Moreover, the analytical solutions presented by Rahmani & Pedram (2014) and Eltaher *et al.* (2012) are utilized for direct comparison. As can be seen from Table 2 to 6, there is a satisfactory agreement between the two sets of results.

Subsequently, a comparison is performed between the current results and the findings of Ref. Nejad & Hadi (2016). In Table 7, the frequency ratios (the ratio of nonlocal linear frequency to classical linear frequency) for CC nanobeam with h = 1 nm, N_x = 0, and N_z = 2 are listed for

Table 3 Comparison of dimensionless fundamental natural frequencies of simply supported nanobeams for N_z = 0.5

L/h	$\eta^2=(e_0a)^2$ $\times10^{-12}$	Non-dimensionless fundamental frequencies $(\widehat{\omega}_1=\omega_1L^2\sqrt{\rho_aA/E_aI})$			
		Present study	Ref. Rahmani & Pedram (2014)	Ref. Eltaher *et al.* (2012)	Numerical model (ABAQUS)
20	0	7.9231	7.7149	7.8061	7.8960
	1	7.5574	7.3602	7.4458	7.5357
	2	7.2381	7.0504	7.1312	7.2212
	3	6.9560	6.7766	6.8533	6.9432
	4	6.7047	6.5325	6.6057	6.6956
	5	6.4787	6.3129	6.3830	6.4728
50	0	7.9167	7.7413	7.7998	7.9005
	1	7.5519	7.3854	7.4403	7.5405
	2	7.2338	7.0745	7.1269	7.2263
	3	6.9527	6.7998	6.8500	6.9488
	4	6.7021	6.5548	6.6031	6.7013
	5	6.4768	6.3345	6.3811	6.4787
100	0	7.9150	7.7451	7.7981	7.9007
	1	7.5511	7.3891	7.4396	7.5412
	2	7.2331	7.0780	7.1263	7.2271
	3	6.9523	6.8032	6.8496	6.9496
	4	6.7018	6.5580	6.6028	6.7021
	5	6.4765	6.3376	6.3808	6.4796

Table 4 Comparison of dimensionless fundamental natural frequencies of simply supported nanobeams for N_z = 1.0

L/h	$\eta^2=(e_0a)^2$ $\times10^{-12}$	Non-dimensionless fundamental frequencies $(\widehat{\omega}_1=\omega_1L^2\sqrt{\rho_aA/E_aI})$			
		Present study	Ref. Rahmani & Pedram (2014)	Ref. Eltaher *et al.* (2012)	Numerical model (ABAQUS)
20	0	7.1896	6.9676	7.0904	7.1638
	1	6.8577	6.6473	6.7631	6.8373
	2	6.5680	6.3674	6.4774	6.5522
	3	6.3122	6.1202	6.2251	6.3004
	4	6.0841	5.8997	6.0001	6.0759
	5	5.8790	5.7014	5.7979	5.8740
50	0	7.1843	6.9917	7.0852	7.1683
	1	6.8529	6.6703	6.7583	6.8418
	2	6.5643	6.3895	6.4737	6.5571
	3	6.3093	6.1414	6.2222	6.3056
	4	6.0818	5.9201	5.9979	6.0812
	5	5.8773	5.7212	5.7962	5.8795
100	0	7.1824	6.9952	7.0833	7.1682
	1	6.8523	6.6736	6.7577	6.8425
	2	6.5637	6.3927	6.4731	6.5578
	3	6.3088	6.1444	6.2217	6.3062
	4	6.0815	5.9231	5.9976	6.0820
	5	5.8771	5.7240	5.7960	5.8803

Table 5 Comparison of dimensionless fundamental natural frequencies of simply supported nanobeams for N_z = 5.0

L/h	$\eta^2=(e_0a)^2$ $\times10^{-12}$	Non-dimensionless fundamental frequencies $(\widehat{\omega}_1=\omega_1L^2\sqrt{\rho_aA/E_aI})$			
		Present study	Ref. Rahmani & Pedram (2014)	Ref. Eltaher *et al.* (2012)	Numerical model (ABAQUS)
20	0	6.1105	5.9172	6.0025	6.0913
	1	5.8286	5.6452	5.7256	5.8144
	2	5.5824	5.4075	5.4837	5.5725
	3	5.3650	5.2702	5.2702	5.3831
	4	5.1711	5.0103	5.0797	5.1683
	5	4.9969	4.8419	4.9086	4.9971
50	0	6.1069	5.9389	5.999	6.0962
	1	5.8247	5.6659	5.7218	5.8187
	2	5.5794	5.4274	5.4808	5.5771
	3	5.3627	5.2166	5.2679	5.3637
	4	5.1694	5.0287	5.078	5.1733
	5	4.9955	4.8597	4.9072	5.0021
100	0	6.1049	5.9421	5.997	6.0959
	1	5.8241	5.6689	5.7212	5.8193
	2	5.5789	5.4302	5.4803	5.5777
	3	5.3623	5.2194	5.2675	5.3643
	4	5.0690	5.0314	5.0777	5.1406
	5	4.9154	4.8623	4.9071	4.9762

Table 6 Comparison of dimensionless fundamental natural frequencies of simply supported nanobeams for N_z = 10.0

L/h	$\eta^2=(e_0a)^2$ $\times10^{-12}$	Non-dimensionless fundamental frequencies $(\widehat{\omega}_1=\omega_1L^2\sqrt{\rho_aA/E_aI})$			
		Present study	Ref. Rahmani & Pedram (2014)	Ref. Eltaher *et al.* (2012)	Numerical model (ABAQUS)
20	0	5.8085	5.6521	5.7058	5.8034
	1	5.5404	5.3923	5.4425	5.5397
	2	5.3064	5.1653	5.2126	5.3094
	3	5.0997	4.9647	5.0096	5.1059
	4	4.9155	4.7858	4.8286	4.9246
	5	4.7498	4.6250	4.6659	4.7615
50	0	5.8027	5.6730	5.7001	5.8065
	1	5.5368	5.4122	5.4389	5.5439
	2	5.3035	5.1843	5.2098	5.3138
	3	5.0975	4.9830	5.0074	5.1106
	4	4.9137	4.8035	4.8269	4.9293
	5	4.7485	4.6421	4.6646	4.7663
100	0	5.8031	5.6760	5.7005	5.8078
	1	5.5362	5.4150	5.4384	5.5445
	2	5.3031	5.1871	5.2094	5.3145
	3	5.0972	4.9857	5.0071	5.1113
	4	4.9135	4.8060	4.8267	4.9300
	5	4.7483	4.6445	4.6644	4.7670

Table 7 Comparison of linear frequency ratios Fr of clamped-clamped BFG nanobeam

L (nm)	Nonlinear frequency ratio ($Fr = \frac{\bar{\omega}}{\bar{\omega}_L}$)							
	μ= 0.1 (nm^2)		μ= 0.5 (nm^2)		μ= 2 (nm^2)		μ= 4 (nm^2)	
	Preset study	Ref. Nejad & Hadi (2016)	Preset study	Ref. Nejad & Hadi (2016)	Preset study	Ref. Nejad & Hadi (2016)	Preset study	Ref. Nejad & Hadi (2016)
10	0.9919	0.9925	0.9686	0.9695	0.8917	0.8925	0.8109	0.8125
20	0.9989	0.9985	0.9913	0.9922	0.9704	0.9712	0.9426	0.9421
30	0.9990	0.9992	0.9975	0.9974	0.9863	0.9871	0.9675	0.9676
40	0.9993	0.9994	0.9987	0.9986	0.9927	0.9926	0.9842	0.9849
50	0.9997	0.9998	0.9997	0.9996	0.9943	0.9947	0.9909	0.9911
60	0.9998	0.9999	0.9999	0.9997	0.9959	0.9962	0.9942	0.9936
70	0.9999	0.9999	0.9999	0.9999	0.9975	0.9971	0.9947	0.9958
80	0.9999	0.9999	0.9999	0.9999	0.9982	0.9974	0.997	0.9965
90	0.9999	0.9999	0.9999	0.9999	0.9991	0.9983	0.9981	0.9976
100	0.9999	0.9999	0.9999	0.9999	0.9998	0.9995	0.9999	0.9988

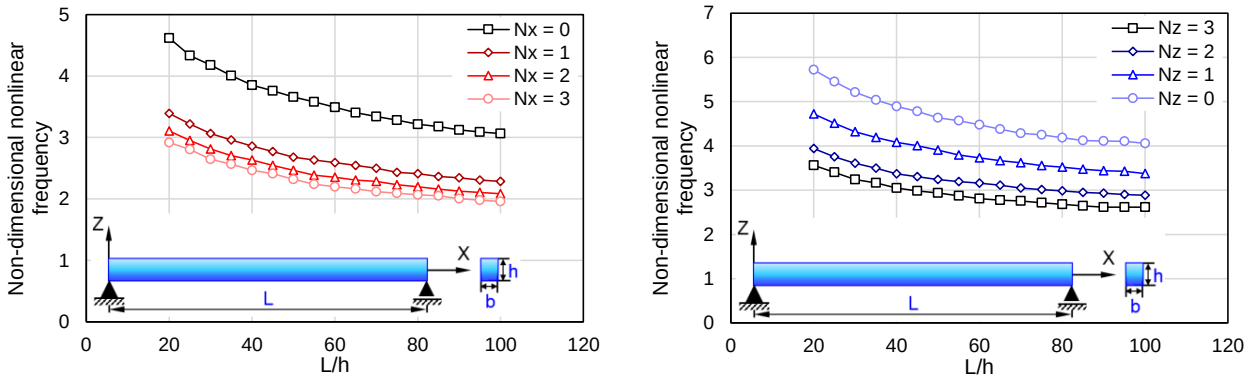

(a) (b)

Fig. 4 Changes in the non-dimensional nonlinear frequency $\bar{\omega}$ of SS FG nanobeams based on $\mathrm{L/h}$ for various amounts of (a) gradient index $\mathrm{N_z}$, when $\mathrm{N_x} = 1$, and (b) gradient index $\mathrm{N_x}$, when $\mathrm{N_z} = 1$

various nonlocal parameters and nanobeam lengths. The analytical solutions provided by Nejad & Hadi (2016) are also given in order to have a direct comparison, as can be clearly inferred from Table 7. Fig. 3 indicates that the present results follow the ones of Nejad & Hadi (2016), and they have little difference.

4.2 Parametric results

This section includes some illustrative numerical examples to investigate how the nonlocal parameter, material distribution, nanobeam length, and boundary conditions can affect the BFG nanobeam's frequency. The cross-sectional dimensions, as well as the material composition of the BFG nanobeam's bottom and top surfaces, have been kept the same as used in Ref. Nejad & Hadi (2016).

In order to clarify how various parameters influence the nonlinear frequency, the obtained results are given based on the dimensionless nonlinear frequency ($\bar{\omega} = \bar{\omega}_L\sqrt{I/A}$) and nonlinear frequency ratio ($F_r = \bar{\omega}/\bar{\omega}_L$). $\bar{\omega}_L$represents the non-dimensional nonlinear frequency when a value of zero is assigned to the nonlocal parameter.

Fig. 4 shows the changes in the non-dimensional nonlinear frequency $\bar{\omega}$ of SS FG nanobeams regarding $\mathrm{L/h}$ for various amounts of N_z and N_x in the case of $\mu = 1\ nm^2$ and $\alpha = 1$. An important point here is that the behavior of the FG beams with CC boundary conditions was analogous to the behavior of the beam with the SS boundary conditions. Hence, the figures for CC boundary conditions are not depicted here to avoid repetition.

As can be clearly seen, with an increase in N_x, $\bar{\omega}$ is reduced, which is because the increment in the gradient index N_x. This would result in a reduction in the effective stiffness of the FG beam and an increase in its effective mass. However, incrementing the gradient index $\mathrm{N_z}$ results in the increment of $\bar{\omega}$. It should be considered that it cannot be concluded that for any values of parameters α, $\mathrm{L/h}$, and μ, increasing $\mathrm{N_z}$ leads to the increase in the $\bar{\omega}$. This is because, with an increase in $\mathrm{N_z}$, both stiffness and mass of the beam would be increased.On the other hand, as can be inferred from mechanical vibration, the vibrational frequency, despite its inverse relationship with stiffness, directly depends on the mass. As a result, the relationship

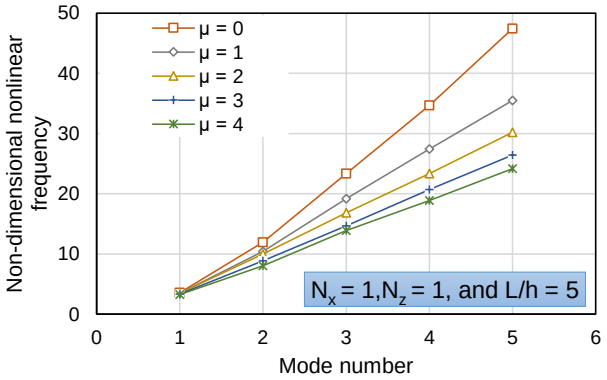

Fig. 5 Changes in the non-dimensional nonlinear frequency $\bar{\omega}$ with changing of the nonlocal parameter for the first five-mode number $N_x=1$, $N_z=1$, and $L/h=5$

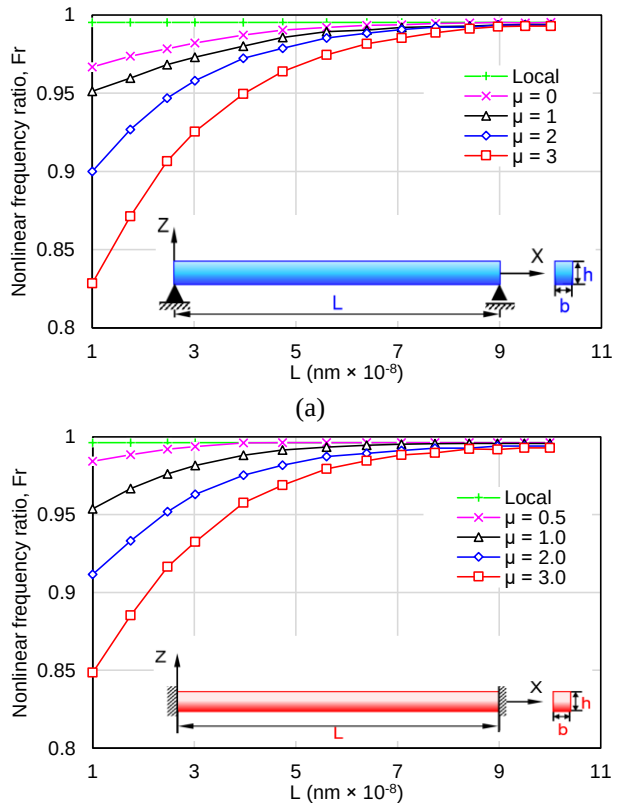

(a)

(b)

Fig. 6 Changes in the nonlinear frequency ratio Fr concerning nanobeam length L for various quantities of the nonlocal parameters μ: (a) SS nanobeam, and (b) CC nanobeam

between $\bar{\omega}$ and N_z can be either direct or inverse. In addition, Fig. 4 shows that the increase in L/h reduces the dimensionless nonlinear frequency, meaning that the nanobeam stiffness decreases with increasing L/h. Moreover, it is obvious that in the case of lower quantities L/h, $\bar{\omega}$ exhibits a more explicit rate of reduction. For example, when N_x=1, if L/h is increased from 20 to 40, then the dimensionless nonlinear frequency will show a reduction of nearly 16%; whereas, increasing L/h from 60 to 80 will lead to a reduction of 5% in the nonlinear frequency ratio (Firouzianhaij *et al.* 2022, Gorji Azandariani *et al.* 2022c, Gorji Azandariani and Gholami 2022b). Fig. 5 depicts the changes in the non-dimensional nonlinear frequency $\bar{\omega}$ for various quantities of the nonlocal parameter and also the first five-mode number. This figure has been plotted for $N_x = 1$, $N_z = 1$, and $L/h = 5$. As can be clearly observed, the impact of the nonlocal parameter on $\bar{\omega}$ increments as the mode number increments. For instance, by incrementing μ from 1 to 2, the 1st mode decreases by 5% while the 5th mode exhibits a reduction of 16%. Fig. 6 illustrates how the nonlinear frequency ratio Fr varies based on the nanobeam's length L. These variations have been plotted for various quantities of the nonlocal parameter μ and also for CC and SS boundary conditions when $N_x = 1$, $N_z = 1$ and $\alpha = 1$.

As can be clearly seen, with an increase in the value of L, the value of Fr is increased as well, which is consistent with the findings of Ref. Nejad & Hadi (2016). It is also inferred from Fig. 6 that the increment of the nonlocal parameter reduces the Fr of the nanobeam. This is because the nonlocal impact causes a reduction in the nanobeam's stiffness. Moreover, Fig. 6 demonstrates that for lower values of L, the parameter Fr exhibits a more obvious dependency on the nonlocal parameter. For example, considering the beam with SS boundary conditions, by increasing the μ from 2 to 3, the Fr exhibits an increase of nearly 5% for $L = 10$ nm, whereas it is increased by merely 2% in the case of $L = 50$ nm.

5. Conclusions

The present work was conducted to evaluate and explore the free vibration behavior of Timoshenko nanobeams made of BFG material. For this purpose, Eringen's nonlocal theory was applied to explore the small-scale effects on free vibration. Also, utilizing the Hamilton principle, the governing partial differential equations and the boundary conditions were determined. The state-space differential equations of the nanobeam were established by employing the variable substitution method; then, the state-space differential equations were applied to construct the dynamic stiffness matrix. In order to calculate the natural frequencies, the Wittrick–Williams algorithm was used as the solution method. Then, the results obtained in this work were compared with those published previously for validation of the present formulation. Also, in the present paper, a detailed discussion was presented on the effects of the nonlocal parameter, material property gradient, nanobeam length, and boundary conditions on the BFG nanobeam's frequency.

The conclusions of the present paper can be summarized as follows:

- The increase of gradient index N_x results in the reduction of dimensionless nonlinear frequency $\bar{\omega}$. However, incrementing the gradient index N_z results in an increased $\bar{\omega}$.

- Increasing the L/h causes a reduction in the $\bar{\omega}$. For lower values of L/h, $\bar{\omega}$ exhibited a more obvious rate of reduction.

- The impact of the nonlocal parameter on $\bar{\omega}$ was shown to be increased with the increase in the mode-shape number.

- Increasing the L results in the increase in the nonlinear frequency ratio F_r for any quantity of the nonlocal parameters.

- When increasing the nonlocal parameter, the F_r of the nanobeam is reduced. For lesser quantities of L, the F_r exhibited a more obvious dependency on the nonlocal parameter.

References

Ahouel, M., Houari, M.S.A., Bedia, E.A.A. and Tounsi, A. (2016), "Size-dependent mechanical behavior of functionally graded trigonometric shear deformable nanobeams including neutral surface position concept", *Steel Compos. Struct.*, **20**(5), 963-981. https://doi.org/10.12989/scs.2016.20.5.963.

Akbaş, Ş.D. (2019), "Hygro-thermal nonlinear analysis of a functionally graded beam", *J. Appl. Comput. Mech.*, **5**(2), 477-485. https://doi.org/10.22055/jacm.2018.26819.1360.

Amar, L.H.H., Kaci, A. and Tounsi, A. (2017), "On the size-dependent behavior of functionally graded micro-beams with porosities", *Struct. Eng. Mech.*, **64**(5), 527. https://doi.org/10.12989/SCS.2017.64.5.527.

Aydogdu, M., Arda, M. and Filiz, S. (2018), "Vibration of axially functionally graded nano rods and beams with a variable nonlocal parameter", *Adv. Nano Res.*, **6**(3), 257-278. https://doi.org/10.12989/anr.2018.6.3.257.

Azandariani, M.G., Gholami, M., Nikzad, A., Azandariani, M.G., Gholami, M. and Nikzad, A. (2022), "Eringen's nonlocal theory for non-linear bending analysis of BGF Timoshenko nanobeams", *Adv. Nano Res.*, **12**(1), 37. https://doi.org/10.12989/ANR.2022.12.1.037.

Bai, Y., Nardi, D.C., Zhou, X., Picón, R.A. and Flórez-López, J. (2021), "A new comprehensive model of damage for flexural subassemblies prone to fatigue", *Comput. Struct.*, **256**, 106639. https://doi.org/10.1016/j.compstruc.2021.106639.

Belarbi, M.O., Houari, M.S.A., Daikh, A.A., Garg, A., Merzouki, T., Chalak, H.D. and Hirane, H. (2021), "Nonlocal finite element model for the bending and buckling analysis of functionally graded nanobeams using a novel shear deformation theory", *Compos. Struct.*, **264**, 113712. https://doi.org/10.1016/j.compstruct.2021.113712.

Berghouti, H., Bedia, E.A.A., Benkhedda, A. and Tounsi, A. (2019), "Vibration analysis of nonlocal porous nanobeams made of functionally graded material", *Adv. Nano Res.*, **7**(5), 351-364. https://doi.org/10.12989/anr.2019.7.5.351.

Chaht, F.L., Kaci, A., Houari, M.S.A., Tounsi, A., Beg, O.A. and Mahmoud, S.R. (2015), "Bending and buckling analyses of functionally graded material (FGM) size-dependent nanoscale beams including the thickness stretching effect", *Steel Compos. Struct.*, **18**(2), 425-442. https://doi.org/10.12989/scs.2015.18.2.425.

Chen, H. and Li, S. (2022), "Collinear nonlinear mixed-frequency ultrasound with FEM and experimental method for structural health prognosis", *Processes*, **10**(4), 656. https://doi.org/10.3390/pr10040656.

Chen, H., Liu, M., Chen, Y., Li, S. and Miao, Y. (2022), "Nonlinear lamb wave for structural incipient defect detection with sequential probabilistic ratio test", *Secur. Commun. Networks*, **2022**. https://doi.org/10.1155/2022/9851533.

Deng, H. and Cheng, W. (2016), "Dynamic characteristics analysis of bi-directional functionally graded Timoshenko beams", *Compos. Struct.*, **141**, 253-263. https://doi.org/10.1016/j.compstruct.2016.01.051.

Ebrahimi, F. and Barati, M.R. (2018), "Stability analysis of functionally graded heterogeneous piezoelectric nanobeams based on nonlocal elasticity theory", *Adv. Nano Res.*, **6**(2), 93-112. https://doi.org/10.12989/anr.2018.6.2.093.

Ebrahimi, F., Fardshad, R.E. and Mahesh, V. (2019), "Frequency response analysis of curved embedded magneto-electro-viscoelastic functionally graded nanobeams", *Adv. Nano Res.*, **7**(6), 391-403. https://doi.org/10.12989/anr.2019.7.6.391.

Ebrahimi, F. and Haghi, P. (2018), "Elastic wave dispersion modelling within rotating functionally graded nanobeams in thermal environment", *Adv. Nano Res.*, **6**(3), 201-217. https://doi.org/10.12989/anr.2018.6.3.201.

Eltaher, M.A., Emam, S.A. and Mahmoud, F.F. (2012), "Free vibration analysis of functionally graded size-dependent nanobeams", *Appl. Math. Comput.*, **218**(14), 7406-7420. https://doi.org/10.1016/j.amc.2011.12.090.

Eringen, A.C. (1983), "On differential equations of nonlocal elasticity and solutions of screw dislocation and surface waves", *J. Appl. Phys.*, **54**(9), 4703-4710. https://doi.org/10.1063/1.332803.

Firouzianhaij, A., Gorji Azandariani, M., Usefi, N. and Samali, B. (2022), "Performance of baseplate connections in CFS storage rack systems: An experimental, numerical and theoretical study", *J. Constr. Steel Res.*, **196**, 107421. https://doi.org/10.1016/j.jcsr.2022.107421.

Gao, Y., Xiao, W. shen, and Zhu, H. (2019), "Nonlinear thermal buckling of bi-directional functionally graded nanobeams", *Struct. Eng. Mech.*, **71**(6), 669-682. https://doi.org/10.12989/sem.2019.71.6.669.

Gholami, M., Zare, E., Gorji Azandariani, M. and Moradifard, R. (2021), "Seismic behavior of dual buckling-restrained steel braced frame with eccentric configuration and post-tensioned frame system", *Soil Dyn. Earthq. Eng.*, **151**, 106977. https://doi.org/10.1016/j.soildyn.2021.106977.

Gorji Azandariani, A., Gholhaki, M. and Gorji Azandariani, M. (2022a), "Assessment of damage index and seismic performance of steel plate shear wall (SPSW) system", *J. Constr. Steel Res.*, **191**, 107157. https://doi.org/10.1016/j.jcsr.2022.107157.

Gorji Azandariani, M., Ghanbari-Ghazijahani, T., Mohebkhah, A. and Classen, M. (2021a), "Concrete- and timber-filled tubes under axial compression - Numerical and theoretical study", *J. Build. Eng.*, **44**, 103231. https://doi.org/10.1016/j.jobe.2021.103231.

Gorji Azandariani, M. and Gholami, M. (2022a), "Seismic fragility investigation of hybrid structures BRBF with eccentric-configuration and self-centering frame", *J. Constr. Steel Res.*, 107300. https://doi.org/https://doi.org/10.1016/j.jcsr.2022.107300.

Gorji Azandariani, M. and Gholami, M. (2022b), "Seismic fragility investigation of hybrid structures BRBF with eccentric-configuration and self-centering frame", *J. Constr. Steel Res.*, **196**, 107300. https://doi.org/10.1016/j.jcsr.2022.107300.

Gorji Azandariani, M., Gholami, M., Vaziri, E. and Nikzad, A. (2021b), "Nonlinear static analysis of a bi-directional functionally graded microbeam based on a nonlinear elastic foundation using modified couple stress theory", *Arab. J. Sci. Eng.*, 1-11. https://doi.org/10.1007/s13369-021-06053-0.

Gorji Azandariani, M., Gholami, M. and Zare, E. (2022b), "Development of spectral element method for free vibration of axially-loaded functionally-graded beams using the first-order shear deformation theory", *Eur. J. Mech. A Solids*, **96**, 104759. https://doi.org/10.1016/j.euromechsol.2022.104759.

Gorji Azandariani, M., Gholhaki, M., Kafi, M.A. and Gorji Azandariani, A. (2022c), "Assessment of cyclic behavior and performance of hybrid linked-column steel plate shear wall

system", *J. Build. Eng.*, **58**, 104963. https://doi.org/10.1016/j.jobe.2022.104963.
Gorji Azandariani, M., Gholhaki, M., Kafi, M.A. and Zirakian, T. (2021c), "Study of effects of beam-column connection and column rigidity on the performance of SPSW system", *J. Build. Eng*., **33** https://doi.org/10.1016/j.jobe.2020.101821.
Gorji Azandariani, M., Kafi, M.A. and Gholhaki, M. (2021d), "Innovative hybrid linked-column steel plate shear wall (HLCS) system: Numerical and analytical approaches", *J. Build. Eng.*, **43**, 102844. https://doi.org/10.1016/j.jobe.2021.102844.
Gu, M., Mo, H., Qiu, J., Yuan, J. and Xia, Q. (2022), "Behavior of floating stone columns reinforced with geogrid encasement in model tests", *Front. Mater.*, Frontiers, **9**, 503. https://doi.org/10.3389/fmats.2022.980851.
Hao, R.B., Lu, Z.Q., Ding, H. and Chen, L.Q. (2022), "A nonlinear vibration isolator supported on a flexible plate: analysis and experiment", *Nonlinear Dyn.*, **108**(2), 941-958. https://doi.org/10.1007/s11071-022-07243-7.
Houari, M.S.A., Bessaim, A., Bernard, F., Tounsi, A. and Mahmoud, S.R. (2018), "Buckling analysis of new quasi-3D FG nanobeams based on nonlocal strain gradient elasticity theory and variable length scale parameter", *Steel Compos. Struct.*, **28**(1), 13-24. https://doi.org/10.12989/scs.2018.28.1.013.
Hu, Z., Shi, T., Cen, M., Wang, J., Zhao, X., Zeng, C., Zhou, Y., Fan, Y., Liu, Y. and Zhao, Z. (2022), "Research progress on lunar and Martian concrete", *Constr. Build. Mater.*, **343**, 128117. https://doi.org/10.1016/j.conbuildmat.2022.128117.
Huang, H., Huang, M., Zhang, W., Pospisil, S. and Wu, T. (2020), "Experimental investigation on rehabilitation of corroded rc columns with BSP and HPFL under combined loadings", *J. Struct. Eng.*, **146**(8), 04020157. https://doi.org/10.1061/(asce)st.1943-541x.0002725.
Huang, H., Huang, M., Zhang, W. and Yang, S. (2021), "Experimental study of predamaged columns strengthened by HPFL and BSP under combined load cases", *Struct. Infrastruct. Eng.*, **17**(9), 1210-1227. https://doi.org/10.1080/15732479.2020.1801768.
Huang, S. and Liu, C. (2022), "A computational framework for fluid-structure interaction with applications on stability evaluation of breakwater under combined tsunami-earthquake activity", *Comput. Civ. Infrastruct. Eng.*, **38**(3), 325-352. https://doi.org/10.1111/mice.12880.
Jia, X.L., Ke, L.L., Feng, C.B., Yang, J. and Kitipornchai, S. (2015), "Size effect on the free vibration of geometrically nonlinear functionally graded micro-beams under electrical actuation and temperature change", *Compos. Struct.*, **133**, 1137-1148. https://doi.org/10.1016/j.compstruct.2015.08.044.
Karami, B. and Janghorban, M. (2019), "On the dynamics of porous nanotubes with variable material properties and variable thickness", *Int. J. Eng. Sci.*, **136**, 53-66. https://doi.org/10.1016/j.ijengsci.2019.01.002.
Karami, B., Shahsavari, D. and Janghorban, M. (2018), "A comprehensive analytical study on functionally graded carbon nanotube-reinforced composite plates", *Aerosp. Sci. Technol.*, Elsevier Masson SAS, **82-83**, 499-512. https://doi.org/10.1016/j.ast.2018.10.001.
Karami, B., Shahsavari, D., Janghorban, M. and Li, L. (2019), "Influence of homogenization schemes on vibration of functionally graded curved microbeams", *Compos. Struct.*, **216**, 67-79. https://doi.org/10.1016/j.compstruct.2019.02.089.
Ke, L.L., Wang, Y.S., Yang, J. and Kitipornchai, S. (2012), "Nonlinear free vibration of size-dependent functionally graded microbeams", *Int. J. Eng. Sci.*, **50**(1), 256-267. https://doi.org/10.1016/j.ijengsci.2010.12.008.
Li, S.R. and Batra, R.C. (2013), "Relations between buckling loads of functionally graded Timoshenko and homogeneous Euler-Bernoulli beams", *Compos. Struct.*, **95**, 5-9. https://doi.org/10.1016/j.compstruct.2012.07.027.
Lim, C.W., Zhang, G. and Reddy, J.N. (2015), "A higher-order nonlocal elasticity and strain gradient theory and its applications in wave propagation", *J. Mech. Phys. Solids*, **78**, 298-313. https://doi.org/10.1016/j.jmps.2015.02.001.
Liu, C., Zhao, Y., Wang, Y., Zhang, T. and Jia, H. (2021), "Hybrid dynamic modeling and analysis of high-speed thin-rimmed gears", *J. Mech. Des. Trans. ASME*, **143**(12) https://doi.org/10.1115/1.4051137.
Luat, D.T., Thom, D. Van, Thanh, T.T., Minh, P. Van, Ke, T. Van, and Vinh, P. Van. (2021), "Mechanical analysis of bi-functionally graded sandwich nanobeams", *Adv. Nano Res.*, **11**(1), 055. https://doi.org/10.12989/ANR.2021.11.1.055.
Nejad, M.Z. (2016), "Hadi A. Eringen's non-local elasticity theory for bending analysis of bi-directional functionally graded Euler-Bernoulli nano-beams", *Int. J. Eng. Sci.*, **106**, 1-9.
Nejad, M.Z. and Hadi, A. (2016), "Non-local analysis of free vibration of bi-directional functionally graded Euler-Bernoulli nano-beams", *Int. J. Eng. Sci.*, **105**, 1-11. https://doi.org/10.1016/j.ijengsci.2016.04.011.
Nejad, M.Z., Hadi, A. and Farajpour, A. (2017), "Consistent couple-stress theory for free vibration analysis of Euler-Bernoulli nano-beams made of arbitrary bi-directional functionally graded materials", *Struct. Eng. Mech.*, **63**(2), 161-169. https://doi.org/10.12989/sem.2017.63.2.161.
Nejad, M.Z., Hadi, A., Omidvari, A. and Rastgoo, A. (2018), "Bending analysis of bi-directional functionally graded Euler-Bernoulli nano-beams using integral form of Eringen's non-local elasticity theory", *Struct. Eng. Mech.*, **67**(4), 417-425. https://doi.org/10.12989/sem.2018.67.4.417.
Niknam, H., Fallah, A. and Aghdam, M.M. (2014), "Nonlinear bending of functionally graded tapered beams subjected to thermal and mechanical loading", *Int. J. Non. Linear. Mech.*, **65**, 141-147. https://doi.org/10.1016/j.ijnonlinmec.2014.05.011.
Rabhi, M., Benrahou, K.H., Kaci, A., Houari, M.S.A., Bourada, F., Bousahla, A.A., Tounsi, A., Bedia, E.A.A., Mahmoud, S.R. and Tounsi, A. (2020), "A new innovative 3-unknowns hsdt for buckling and free vibration of exponentially graded sandwich plates resting on elastic foundations under various boundary conditions", *Geomech. Eng.*, **22**(2), 119-132. https://doi.org/10.12989/gae.2020.22.2.119.
Rahmani, O. and Pedram, O. (2014), "Analysis and modeling the size effect on vibration of functionally graded nanobeams based on nonlocal Timoshenko beam theory", *Int. J. Eng. Sci.*, **77**, 55-70. https://doi.org/10.1016/j.ijengsci.2013.12.003.
Rahmani, O., Refaeinejad, V. and Hosseini, S.A.H. (2017), "Assessment of various nonlocal higher order theories for the bending and buckling behavior of functionally graded nanobeams", *Steel Compos. Struct.*, **23**(3), 339-350. https://doi.org/10.12989/scs.2017.23.3.339.
Rousta, A.M. and Azandariani, M.G. (2022), "Micro-finite element and analytical investigations of seismic dampers with steel ring plates", *Steel Compos. Struct.*, **43**(5), 565. https://doi.org/10.12989/SCS.2022.43.5.565.
Rousta, A.M., Shojaeifar, H., Azandariani, M.G., Saberiun, S. and Abdolmaleki, H. (2021), "Cyclic behavior of an energy dissipation semi-rigid moment steel frames (SMRF) system with LYP steel curved dampers", *Struct. Eng. Mech.*, **80**(2), 129. https://doi.org/10.12989/SEM.2021.80.2.129.
Sanjay Anandrao, K., Gupta, R.K., Ramchandran, P. and Venkateswara Rao, G. (2012), "Non-linear free vibrations and post-buckling analysis of shear flexible functionally graded beams", *Struct. Eng. Mech.*, **44**(3), 339-361. https://doi.org/10.12989/sem.2012.44.3.339.
Setoodeh, A.R. and Rezaei, M. (2017), "Large amplitude free vibration analysis of functionally graded nano/micro beams on nonlinear elastic foundation", *Struct. Eng. Mech.*, **61**(2), 209-

220. https://doi.org/10.12989/sem.2017.61.2.209.

Shan, Y., Zhao, J., Tong, H., Yuan, J., Lei, D. and Li, Y. (2022), "Effects of activated carbon on liquefaction resistance of calcareous sand treated with microbially induced calcium carbonate precipitation", *Soil Dyn. Earthq. Eng.*, **161**, 107419. https://doi.org/10.1016/j.soildyn.2022.107419.

Shi, L., Xiao, X., Wang, X., Liang, H. and Wang, D. (2022), "Mesostructural characteristics and evaluation of asphalt mixture contact chain complex networks", *Constr. Build. Mater.*, **340**, 127753. https://doi.org/10.1016/j.conbuildmat.2022.127753.

Şimşek, M. (2014), "Large amplitude free vibration of nanobeams with various boundary conditions based on the nonlocal elasticity theory", *Compos. Part B Eng.*, **56**, 621-628. https://doi.org/10.1016/j.compositesb.2013.08.082.

Şimşek, M. (2016), "Nonlinear free vibration of a functionally graded nanobeam using nonlocal strain gradient theory and a novel Hamiltonian approach", *Int. J. Eng. Sci.*, **105**, 12-27. https://doi.org/10.1016/j.ijengsci.2016.04.013.

Simsek, M. and Yurtcu, H.H. (2013), "Analytical solutions for bending and buckling of functionally graded nanobeams based on the nonlocal Timoshenko beam theory", *Compos. Struct.*, **97**, 378-386. https://doi.org/10.1016/j.compstruct.2012.10.038.

Tagrara, S.H., Benachour, A., Bouiadjra, M.B. and Tounsi, A. (2015), "On bending, buckling and vibration responses of functionally graded carbon nanotube-reinforced composite beams", *Steel Compos. Struct.*, **19**(5), 1259-1277. https://doi.org/10.12989/scs.2015.19.5.1259.

Talebizadehsardari, P., Eyvazian, A., Gorji Azandariani, M., Nhan Tran, T., Kumar Rajak, D. and Babaei Mahani, R. (2020), "Buckling analysis of smart beams based on higher order shear deformation theory and numerical method", *Steel Compos. Struct.*, **35**(5), 635-640. https://doi.org/https://doi.org/10.12989/scs.2020.35.5.635.

Thai, H.T. and Vo, T.P. (2012), "Bending and free vibration of functionally graded beams using various higher-order shear deformation beam theories", *Int. J. Mech. Sci.*, **62**(1), 57-66. https://doi.org/10.1016/j.ijmecsci.2012.05.014.

Usefvand, M., Rousta, A.M., Azandariani, M.G. and Abdolmaleki, H. (2021), "Steel dual-ring dampers: Micro-finite element modelling and validation of cyclic behavior", *Smart Struct. Syst.*, **28**(4), 579. https://doi.org/10.12989/SSS.2021.28.4.579.

Vaziri, E., Gholami, M. and Gorji Azandariani, M. (2021), "The Wall-Frame Interaction Effect in Corrugated Steel Plate Shear Walls Systems", *Int. J. Steel Struct.*, **21**(5), 1680-1697. https://doi.org/10.1007/s13296-021-00529-3.

Wang, J.F., Cao, S.H. and Zhang, W. (2021), "Thermal vibration and buckling analysis of functionally graded carbon nanotube reinforced composite quadrilateral plate", *Eur. J. Mech. A Solids*, **85**, 104105. https://doi.org/10.1016/j.euromechsol.2020.104105.

Wei, J., Xie, Z., Zhang, W., Luo, X., Yang, Y. and Chen, B. (2021), "Experimental study on circular steel tube-confined reinforced UHPC columns under axial loading", *Eng. Struct.*, **230**, 111599. https://doi.org/10.1016/j.engstruct.2020.111599.

Yang, F., Chong, A.C.M., Lam, D.C.C. and Tong, P. (2002), "Couple stress based strain gradient theory for elasticity", *Int. J. Solids Struct.*, **39**(10), 2731-2743. https://doi.org/10.1016/S0020-7683(02)00152-X.

Yuan, J., Lei, D., Shan, Y., Tong, H., Fang, X. and Zhao, J. (2022), "Direct shear creep characteristics of sand treated with microbial-induced calcite precipitation", *Int. J. Civ. Eng.*, **20**(7), 763-777. https://doi.org/10.1007/s40999-021-00696-8.

Zenkour, A.M. and Abouelregal, A.E. (2015), "Thermoelastic interaction in functionally graded nanobeams subjected to time-dependent heat flux", *Steel Compos. Struct.*, **18**(4), 909-924. https://doi.org/10.12989/scs.2015.18.4.909.

Zhang, C., Mousavi, A.A., Masri, S.F., Gholipour, G., Yan, K. and Li, X. (2022a), "Vibration feature extraction using signal processing techniques for structural health monitoring: A review", *Mech. Syst. Signal Process.*, **177**, 109175. https://doi.org/10.1016/j.ymssp.2022.109175.

Zhang, H., Liu, Y. and Deng, Y. (2021), "Temperature gradient modeling of a steel box-girder suspension bridge using Copulas probabilistic method and field monitoring", *Adv. Struct. Eng.*, **24**(5), 947-961. https://doi.org/10.1177/1369433220971779.

Zhang, W., Liu, X., Huang, Y. and Tong, M.N. (2022b), "Reliability-based analysis of the flexural strength of concrete beams reinforced with hybrid BFRP and steel rebars", *Arch. Civ. Mech. Eng.*, **22**(4), 171. https://doi.org/10.1007/s43452-022-00493-7.

Zhou, X., Bai, Y., Nardi, D.C., Wang, Y., Wang, Y., Liu, Z., Picón, R.A. and Flórez-López, J. (2022), "Damage evolution modeling for steel structures subjected to combined high cycle fatigue and high-intensity dynamic loadings", *Int. J. Struct. Stab. Dyn.*, **22**(3), 2240012. https://doi.org/10.1142/S0219455422400120.

Zhu, X. Q. and Law, S.S. (2001), "Precise time-step integration for the dynamic response of a continuous beam under moving loads", *J. Sound Vib.*, **240**(5), 962-970. https://doi.org/10.1006/jsvi.2000.3184.

Zidi, M., Houari, M.S.A., Tounsi, A., Bessaim, A. and Mahmoud, S.R. (2017), "A novel simple two-unknown hyperbolic shear deformation theory for functionally graded beams", *Struct. Eng. Mech.*, **64**(2), 145-153. https://doi.org/10.12989/sem.2017.64.2.145.

JL